



Technical-economic analysis of the insertion of PV power into a wind-solar hybrid system

Diego B. Carvalho*, Eduardo C. Guardia, José W. Marangon Lima

Institute of Electrical and Energy Systems, Federal University of Itajubá, BPS Av., 1303, 37500-903 Itajubá, MG, Brazil

ARTICLE INFO

Keywords:

Wind energy

Solar energy

Hybrid energy systems

Technical-economic analysis

ABSTRACT

In order to mitigate the lack of energy production, several types of energy sources have been combined in a so-called hybrid energy system; however, some economic analysis must be performed to evaluate whether the hybrid business is financially feasible. This work aims to evaluate wind-PV hybrid systems technical and economically through the simulation of a hypothetical hybrid power plant in which a case study is presented. The economic viability of PV power into wind systems is assessed by the comparison of distinct scenarios, which consider different rated power for each type of source. The paper regards the context of the Brazilian energy market and is geared toward the rules, the current tariff prices, and the mean investment applied for the construction of wind and PV systems in Brazil nowadays. The results show that a pure wind energy system is economically ideal and the continuous insertion of PV power into the wind system decreases the chances of profitability. However, for certain amount of PV rated power installed in the complex, the project maintains a high probability of being successful.

1. Introduction

Recently, there have been interest in energy production through renewables worldwide not only because of the use of renewable sources providing positive environmental externalities and sustainability (see Middleton, 2018), but also because they can bring significant macro-economic results, that is, they somehow influence the economic development of a nation by causing some impacts on gross domestic product, unemployment, and balance of trade, to name but a few (Andini et al., 2019). Although renewable energy technologies can be costly (Krozer, 2013), one of the main issues related to these types of sources is about their intermittent feature that does not allow them to produce energy steadily. Wind and PV power sources are included and generate electricity only if natural resources are available abundantly and locally. Thus, energy planning requires accurate information about weather and local resources since investors, risk capital enterprises, and independent energy producers tend to avoid risky projects where reliable data are not disposable (Martins et al., 2007).

To mitigate the risks associated with the fluctuation of power generation by renewables such as wind and PV, an alternative that is being widely used in academic field is the integration of different renewable sources into a single set so-called hybrid energy system. Two or more

energy sources are connected to each other through substations and all of them generate and provide power flow to the power grid. Many studies on hybrid energy arrangements have been conducted addressing general issues about solar-wind systems (Ding et al., 2019; Huang et al., 2015; Ishaq et al., 2018). Some of them are geared toward technical-economic analysis (Aguilar-jiménez et al., 2018). Wind and solar sources are transforming electrical power throughout the world (Syed, 2017). PV systems require low cost for maintenance, are easy to install, but are expensive as compared to wind energy systems, which, in turn, require expertise to operate and are cheap only on a large scale Syed (2017). One of the greatest advantages of combining those types of sources is that the complementary nature of each one can reduce impacts of intermittency Syed (2017) and therefore allow the hybrid system to produce power constantly.

Despite this benefit, there are some other aspects that influence the project of a hybrid energy system economically and investors must be aware of them before applying capital for such business. In order to assess financially an integration of wind and PV systems into a single hybrid set, NPV is applied while MCS is performed not only to represent the stochastic nature of some variables considered in this work such as wind speed and solar irradiation but also to quantify the economic risk of wind-solar systems projects. With respect to the MCS approach, many

Abbreviations: PV, photovoltaic; NPV, net present value; MCS, monte carlo simulation; STC, standard test conditions; pdf, probability density function; MERRA, Modern Era Retrospective-Analysis for Research and Applications; *cf.*, capacity factor

* Corresponding author.

E-mail addresses: diego@unifei.edu.br (D.B. Carvalho), eduardo.guardia@unifei.edu.br (E.C. Guardia), marangon@unifei.edu.br (J.W. Marangon Lima).

<https://doi.org/10.1016/j.solener.2019.06.070>

Received 6 February 2019; Received in revised form 26 June 2019; Accepted 27 June 2019

Available online 16 September 2019

0038-092X/ © 2019 International Solar Energy Society. Published by Elsevier Ltd. All rights reserved.

Nomenclature

| | |
|----------------------|--|
| α | performance ratio (dimensionless parameter) |
| γ | cell maximum power temperature coefficient ($^{\circ}\text{C}^{-1}$) |
| i^{pv} | investment per PV rated power (US\$/MW) |
| i^{wind} | investment per wind rated power (US\$/MW) |
| ρ | air density (kg/m^3) |
| φ | annual degradation rate (%) |
| A | area swept by the wind turbine blades (m^2) |
| c | scale parameter (m/s) |
| $c_{O\&M}^{pv}$ | PV annual operating and maintaining cost per MW (US \$/MW) |
| $c_{O\&M}^{wind}$ | wind annual operating and maintaining cost per MW (US \$/MW) |
| C_p | power coefficient (dimensionless parameter) |
| cf_{annual}^{pv} | capacity factor of PV farms (%) |
| cf_{annual}^{wind} | capacity factor of wind power plants (%) |
| E_{annual}^{wind} | annual energy produced through wind turbines(MWh) |
| $E_{pv(annual)}$ | energy generated by the PV array annually (MWh) |
| $E_{pv(n)}$ | energy generated by the PV array monthly (MWh) |
| E_{pv} | total energy provided by the PV array over a period of time (MWh) |
| $E_{wind(n)}$ | monthly energy produced through wind turbines(MWh) |
| G | incident global irradiance ($\frac{\text{W}}{\text{m}^2}$) |

| | |
|-------------------|---|
| G_n | incident global irradiance in STC ($\frac{\text{W}}{\text{m}^2}$) |
| h | insolation time (hours) |
| I | initial investment cost (US\$) |
| i | discount rate (%) |
| k | period of analysis (years) |
| L | Location parameter |
| n | certain month of the useful life of the equipment (month) |
| N_p | number of PV panels connected in parallel |
| N_s | number of PV panels connected in series |
| NPV | Net Present Value (US\$) |
| P_N^{pv} | PV rated power (MW) |
| P_N^{wind} | wind rated power (MW) |
| P_{pv} | cell output power (W) |
| P_{wind} | wind turbine output power (W) |
| r | monthly degradation rate (%) |
| T | cell temperature ($^{\circ}\text{C}$) |
| t_n | time in which wind turbines keep functioning in the n -th month (hours) |
| T_{amb} | environmental temperature ($^{\circ}\text{C}$) |
| $T_{c,NOCT}$ | nominal operating cell temperature ($^{\circ}\text{C}$) |
| V_u | wind speed (m/s) |
| $W(V_u, z, c, L)$ | Weibull distribution function |
| z | shape parameter (a dimensionless parameter) |

academic works in solar energy field (Blanco et al., 2014; Gu et al., 2018; Kim et al., 2019; Shadmehri et al., 2018) have applied this tool in order to evaluate variables that behave randomly. Furthermore, MCS is also employed in papers that deal with economic issues related to renewable energy projects (Aquila et al., 2017; Feretic and Tomsic, 2005; Heck et al., 2016).

Aquila et al. (2016) study the impact of incentive strategies on the financial risk of wind power generation projects in Brazil in different marketing environments. They employ the NPV method and a stochastic approach to assess the work purposes. The results found showed that the project viability probability is greater than 85% in all scenarios evaluated. Rout et al. (2018) evaluate the economic risk of domestic solar water heaters in India applying the net present value tool and the MCS approach. The research allowed the authors to find out that solar water heaters are only feasible for certain regions of India. Pillot et al. (2018) have conducted analysis of distributed PV generation in Brazil by using a probabilistic Monte Carlo tool. It was found out that the economic viability of many residential PV systems in southern Brazil is not guaranteed mainly due to low nominal capacity of the region.

In relation to hybrid energy systems, Al-ghussain et al. (2017) study a hybrid PV/wind system with energy storage from bank of batteries. The results show that systems with batteries are economically more feasible than systems without energy storage systems. Daigavane and Fulzele (2018) present the design of an optimized hybrid renewable energy system consisting of PV and wind generator with battery. The research found the most suitable solution for hybrid system. Spuru and Lizica-simona (2018) conduct a technical and economic analysis of a PV/wind/diesel hybrid power system in the south-eastern part of Romania, in a remote area with good potential of wind and solar resources. The results show a renewable energy use rate of 65% and a generating cost of electricity of 0.118 €/kWh.

This work seeks to assess the economic viability of wind-PV hybrid systems generating power for trading. The paper regards the Brazilian market context taking account of the tariff prices in which the energy is sold nationally, as well as the mean investment cost of wind power plants and PV arrangements often offered in the energy market. Furthermore, the insertion of PV power into a wind power plant is analyzed by some scenarios, which present different proportions of wind-and-PV-rated-power. This analysis is performed to compare these

types of sources in terms of the financial return that each provides to investors. In order to accomplish the purpose of this article, a wind-PV hybrid complex sited in northeastern Brazil and comprising a 21.6 MW-rated-power-wind-plant and a 4.8 MW-rated-power-PV-farm is utilized as case study. Much information on this hybrid power plant is taken into consideration so that the simulation through mathematical models may be performed more faithfully to reality.

The structure of this article is as follows. The next section, Section 2, presents a brief summary of wind and photovoltaic sources focusing on the output power mathematical modeling thereof. Section 3 addresses subjects related to the wind speed and solar irradiation data collection, as well as economic models used in this work as evaluation methodologies. Section 4 presents the Brazilian energy market pointing out the auctions as means of energy trade and citing the hybrid energy production in Brazil currently. Section 5 shows the case study, scenarios and some results found in this study. Finally, some final comments are presented in the Section 6.

2. Wind and PV power systems

2.1. Wind sources: wind power modeling

Since revenues are obtained from power generation, it is important to know the mathematical modeling of wind and PV power output. By this modeling, we can know how much of power have been produced and, thus, infer how much of annual revenues are being generated. Some information about wind and PV power modeling are presented in the next subsections. The following steps are conducted and lead us toward the wind power mathematical model.

The image depicted in Fig. 1 presents the wind flow through a wind turbine. The wind has high speed upstream, that is, right before passing through the turbine blades. When the wind crosses the rotor, it dampens and decreases its speed downstream. This is in accordance with the law of conservation of energy, since the loss of kinetic energy by the wind implies that electric power is being generated. In the following picture, as well as in the equations presented forward, V_u , V_d , and V are the wind speeds upstream, downstream, and through the rotor blades, respectively, whereas A_u , A_d , and A are the sectional areas crossed by the wind flow upstream, downstream, and through the rotor blades,

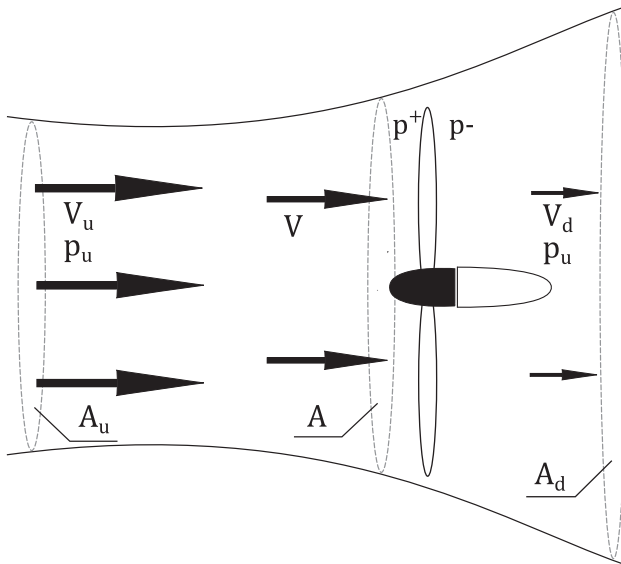


Fig. 1. Wind through turbine blades.

respectively. The following equations are mentioned according to Kulunk (2011) and result in the formula of the wind turbine output power largely employed in several academic researches.

Since there is no loss of mass by the wind when it passes through the imaginary duct, the Eq. (1) can be applied:

$$\dot{m} = \rho A_u V_u = \rho A_d V_d = \rho A V = \text{constant} \quad (1)$$

where ρ is the air density.

The wind speed through the turbine rotor is related to the speed upstream by the variable a .

$$V = V_u \cdot (1 - a) \quad (2)$$

From Eq. (1) and Eq. (2), we can write:

$$A = \frac{A_u}{1 - a} \quad (3)$$

The reduction of the wind speed represents a momentum variation in the air flow, which is caused by the force exerted by the pressure variation in the turbine rotor. Mathematically, this can be written as follows:

$$\underbrace{\Delta v \cdot \dot{m}}_{\Delta v} = \underbrace{\Delta p \cdot A}_{\Delta p} \quad (4)$$

Applying Bernoulli equation to both sections of the imaginary duct:

$$\frac{1}{2} \rho V_u^2 + \rho_u g h_u = \frac{1}{2} \rho V^2 + \rho g h + p^+ \quad (5)$$

Considering the fluid is incompressible and the system is horizontal, we could write:

$$\begin{cases} \frac{1}{2} \rho V_u^2 + p_u = \frac{1}{2} \rho V^2 + p^+ \\ \frac{1}{2} \rho V_d^2 + p_u = \frac{1}{2} \rho V^2 + p^- \end{cases} \quad (6)$$

Subtracting both equations above, we have Eq. (7).

$$p^+ - p^- = \frac{1}{2} \rho (V_u^2 - V_d^2) \quad (7)$$

Putting Eq. (7) into Eq. (4), we obtain Eq. (8).

$$V_d = (1 - 2a) V_u \quad (8)$$

The force applied by the wind to the turbine rotor is given by Eq. (9).

$$F = (p^+ - p^-) A = 2 \rho A V_u^2 a (1 - a) \quad (9)$$

The power P is given then by Eq. (10).

$$P = FV = 2 \rho A V_u^3 a (1 - a)^2 \quad (10)$$

Finally, the wind turbines output power can be expressed by Eq. (11). This equation is employed in many works in the literature related to simulations of wind power production (Lamas, 2017; Syed, 2017; Wais, 2017; Yan and Ouyang, 2018).

$$P_{wind} = \frac{1}{2} C_p \rho A V_u^3 \quad (11)$$

where ρ is the air density (kg/m^3), A is the area swept by the rotor blades (m^2), V_u is the wind speed (m/s), and C_p is the turbine power coefficient (dimensionless parameter).

The C_p parameter can be obtained by the following formula: $C_p = 4 \cdot a \cdot (1 - a)^2$ as it is possible to infer by comparing Eqs. (10) and (11). Aquila et al., 2016; however, suggest a function from a cubic regression for the C_p calculation in terms of the wind speed rather than the a variable. Eq. (12) provides the value of C_p for each value of wind speed considered.

$$C_p = -0,08114 + 0,1771V_u - 0,01539V_u^2 + 0,00034V_u^3 \quad (12)$$

The energy generated by wind turbines is simulated through Eq. (13). It simulates the monthly energy generated and sold by wind power plant investors. The n parameter indicates the month of the year in which the energy is being achieved. Eq. (14), in turn, shows the calculation of the annual energy generated along a year by summing the energy obtained in each month.

$$E_{wind(n)} = P_{wind} * t_n \quad (13)$$

where $E_{wind(n)}$ is the monthly energy provided by wind turbines (MWh) and t_n corresponds to the time (hours) that windmills keep running. Since wind turbines do not stop working throughout the year and considering a monthly length of time, t_n is assumed to be equal to the product of 24 hours and the number of days of the n -month.

$$E_{annual}^{wind} = \sum_{n=1}^{12} E_{wind(n)} \quad (14)$$

where E_{annual}^{wind} is the annual energy generated by wind power plants (MWh).

The capacity factor (cf) measures the cost-effectiveness of energy sources, which matters for cost calculations and for the carbon reduction targets (Boccard, 2009). It corresponds to the ratio between the power indeed provided by the energy source and the power that this same source would generate if it were constantly running at maximum power. The capacity factor of a power generation unit depends basically on both the technological level of the power source's equipment – modern apparatus is able to generate larger amount of energy – and the area where the source is built – the availability or lack of natural resources surround the region influences the production of power by renewables.

The annual capacity factor of wind power plants may be calculated by the following formula presented in Eq. (15).

$$cf_{annual}^{wind} = \sum_{n=1}^{12} \frac{E_{wind(n)}}{P_N^{wind} \times t_n} \quad (15)$$

2.2. PV systems: PV power modeling

A PV system converts sunlight irradiation into electrical power. The tool responsible for this conversion is PV cells, which are semiconductor diodes made through different processes. There are several kinds of material utilized in PV cells manufacturing; however, silicon is the most common. A silicon wafer is connected to electric terminals, and a circuit is formed. When the sunlight reaches the PV surface, the cells generate

charge carriers and produce electric current that flows through the short-circuit (Villalva et al., 2009).

Manufacturers provide ratings for PV modules for conditions referred to STC, achieving results by indoor solar simulators (Fuentes et al., 2007). Some of those conditions include global irradiance of $1000 \frac{W}{m^2}$ and a PV module temperature of $25^\circ C$ Fuentes et al. (2007). The mathematical model of the PV output power is in line with these parameters as shown further.

One of the simplest PV cell models is employed in this work in order to simulate the output power of PV arrays. The sketch of this model is presented in Fig. 2a and comprises a single diode connected to a series resistance, R_s . The power provided by PV cells of such model is given by Eq. (16) (Lorenzo, 1994).

$$P_{max} = V_{oc} I_{sc} FF \tag{16}$$

where P_{max} is the maximum output power delivered by photovoltaic cells. V_{oc} and I_{sc} are, respectively, the open circuit voltage and the short circuit current of PV cells and FF is the fill factor.

The maximum power provided by PV cells is found by the product of the current I_m and the voltage V_m shown in the PV cell curve – Fig. 2b. However, it is rather convenient to use V_{oc} and I_{sc} to estimate the maximum power of cells, and, for this purpose, FF is utilized. Alramlawi et al. (2017) mention that FF is the quotient of the maximum power that is generated by PV cells to the product of the open circuit voltage and the short circuit current thereof. Mathematically, it may be written as $FF = \frac{V_m I_m}{V_{oc} I_{sc}}$. V_{oc} and I_{sc} are dependent on the solar irradiance as well as the temperature of the PV cell (Alramlawi et al., 2017) and are calculated according to the following equations.

$$V_{oc} = V_{oc}^* + \beta_v (T - 25) \tag{17}$$

where V_{oc}^* is the open circuit voltage of PV cells under standard test conditions (V), β_v is the temperature coefficient of PV cells referent to the open circuit voltage, and T is the cell temperature ($^\circ C$).

$$I_{sc} = \frac{G}{G_n} (I_{sc}^* + \beta_i (T - 25)) \tag{18}$$

where G and G_n are the incident solar irradiance and the incident solar irradiance under standard test conditions ($\frac{W}{m^2}$), respectively. G_n is assumed to be equal to $1000 \frac{W}{m^2}$. I_{sc}^* is the short circuit current of PV cells under standard test conditions (A), and β_i is the temperature coefficient of PV cells referent to the short circuit current.

Therefore, the maximum output power provided by a PV cell can be calculated as a product of the right-hand side of the Eqs. (17) and (18) and the fill factor FF . However, since the calculation of the presented current and voltage involves several different parameters, many mathematical models for the estimation of PV output power have been proposed in the literature. One of the simplest is shown by Osterwald whose formula is presented through Eq. (19) and thoroughly described in Osterwald (1986). The Osterwald’s model maintains some similarity

in relation to the result obtained from the application of Eq. (16), although some differences are perceptible. Nonetheless, because of its simplicity and accuracy as well as the easiness of finding the parameters thereof in the manufacturers’ data sheet, the Osterwald’s model has been widely applied to several works published previously (Almeida et al., 2017; Fernández et al., 2013; Marion, 2002).

$$P_{pv} = P_{STC} \cdot \frac{G}{G_n} \left[1 - \gamma \cdot (T - 25) \right] \tag{19}$$

where P_{pv} is the cell maximum power (W), P_{STC} is the cell maximum power under standard test conditions, and γ is the cell maximum power temperature coefficient ($^\circ C^{-1}$).

To find the cell temperature, T , some mathematical models can be found in the literature. Barbieri et al. (2016), for example, present lots of those models and states that the Ross-Smokler’s modeling (Ross and Smokler, 1986) for T estimation is one of the most common used in researches. Eq. (20) shows the Ross-Smokler model.

$$T = T_{amb} + \frac{G}{G_{NOCT}} \cdot (T_{c,NOCT} - T_{NOCT}) \tag{20}$$

where T_{amb} is the environmental temperature ($^\circ C$), $T_{c,NOCT}$ is the nominal operating cell temperature ($^\circ C$) provided by the manufacturer, G_{NOCT} is assumed to be equal to $800 \frac{W}{m^2}$ (Barbieri et al., 2016), and T_{NOCT} is equal to $20^\circ C$ (Barbieri et al., 2016).

In addition to the presented formulas, Eq. (21) estimates the energy provided by PV cells, which is one of the most valuable formulas shown in this paper since energy is the product that is sold by investors. Therefore, Eq. (21) is crucial for the great accomplishment of this work’s purpose and has been used in some published paper such as in Rocha et al. (2017).

$$E_{pv} = P_{pv} \cdot h \cdot \alpha \cdot N_s \cdot N_p \tag{21}$$

where E_{pv} is the energy provided by the PV array over a period of time (Wh), h is the insolation time (hours), α is the performance ratio (dimensionless parameter), N_s is the number of PV panels connected in series, and N_p is the number of PV panels connected in parallel.

The energy equation shows us the α parameter that is considered because PV arrays are unsuccessful in converting all energy received from the sun into electricity. During the conversion, only some part of the sunlight energy is transformed in electric power, and it occurs due to the losses in the inverters, shading, dust and dirt on modules. An α equal to 81% is taken according to Elilob et al. (2016).

Rocha et al. (2017) still states that an annual degradation rate, φ , of 0.8% must be considered since the panels’ cells wear out over time. Since the energy is traded monthly, φ is converted to a monthly degradation rate, r , by the following equation:

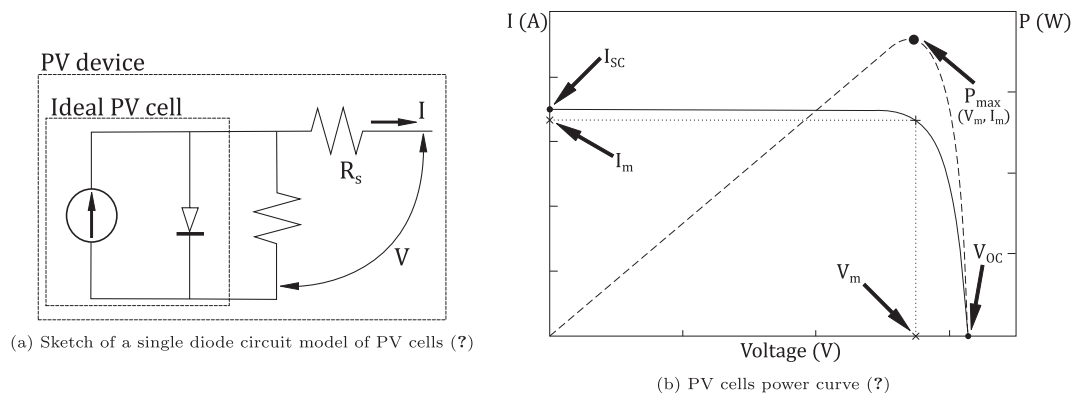


Fig. 2. PV cells power circuit and curve.

$$r = - \left[(1 - \varphi)^{\left(\frac{1}{12}\right)} - 1 \right] \tag{22}$$

where r is the monthly degradation rate (%).

Thus, the monthly energy produced by the PV array can be found through Eq. (23)

$$E_{pv(n)} = E_{pv} \times (1 - r)^n \tag{23}$$

where $E_{pv(n)}$ is the energy generated by the PV array monthly (MWh) and n is the n -month of the useful life of the equipment (month).

To calculate the annual energy generated by the PV array, we utilize Eq. (24).

$$E_{annual}^{pv} = \sum_{n=1}^{12} E_{pv(n)} \tag{24}$$

Just as the capacity factor of wind power plants is calculated through Eq. (15), so the capacity factor of PV farms is obtained through Eq. (25).

$$cf_{annual}^{pv} = \sum_{n=1}^{12} \frac{E_{pv(n)}}{P_N^{pv} \times t_n} \tag{25}$$

3. Data collection and financial arrangements

3.1. Wind speed and solar irradiation data attainment

Among several global reanalysis datasets from meteorological models available, MERRA has been widely employed because it has a high temporal and spatial resolution (Olauson and Bergkvist, 2015) and also because it can be easily and free accessed by researchers (Boilley and Wald, 2015). Indeed, MERRA is largely used in works of various domains: oceanography, climate, energy production, life cycle analysis, agriculture, ecology, human health, and air quality (Lefèvre et al., 2014). MERRA is a set of ground, atmosphere, and aerosol products for the modern satellite era managed by NASA (Xi et al., 2019) and has been used since 1979 until the present day. Although the datasets utilized in reanalysis are accurate in relation to those stemmed from predictions, there are still uncertainties (Olauson and Bergkvist, 2015).

Another reanalysis model that has been used in many published works, especially those focused on solar irradiation dataset, is HelioClim-1. HelioClim-1 is the result of a project launched in 1997 and comprises several databases that cover many regions around the globe. These databases utilize satellite images as inputs for their creation and updating (Boilley and Wald, 2015). It can be accessed by the following Web address: www.soda-is.com (Boilley and Wald, 2015). The website requires the geographical coordinates of the site where the dataset shall be obtained.

In this paper, MERRA and HelioClim-1 are used so that wind speed and solar irradiation datasets of a specific site are collected. The sets comprise hourly data, which are utilized to specify the input parameters of the MCS. The site from where the data are collected is part of the case study proposed in this work and hosts a prototype of a wind-solar hybrid energy system.

3.2. Net present value and Monte Carlo simulation

Net present value can be expressed as the difference between the present value of cash inflows and outflows. It compares the value of current investments to the future value of the money based on the discount rate. NPV is one of the most preferred techniques to evaluate the profitability of projects (Lee et al., 2016). Positive values of NPV imply a feasible investment and can be calculated by the Eq. (26).

$$NPV = -I + \sum_{x=1}^k \frac{C_x}{(1 + i)^x} \tag{26}$$

where I is the initial investment cost (US\$), C_x is the cash flow at k -th year (US\$), k is the period of analysis (years), and i is the discount rate (%).

The initial investment cost, as well as the C_x are calculated according to the following equations:

$$I = (I^{wind} \times P_N^{wind}) + (I^{pv} \times P_N^{pv}) \tag{27}$$

where I^{wind} and I^{pv} are the investment per MW of wind and PV rated power (US\$/MW), respectively, while P_N^{wind} and P_N^{pv} are the wind and the PV rated power (MW), respectively.

$$C_x = R_{annual} - Costs_{annual} \tag{28}$$

The R_{annual} parameter is the annual revenue calculated through the wind and the photovoltaic energy sold by the prices λ^{wind} and λ^{pv} , respectively, as shown by Eq. (29). Both parameters are given in US \$/MWh.

$$R_{annual} = (E_{annual}^{wind} \times \lambda^{wind}) + (E_{annual}^{pv} \times \lambda^{pv}) \tag{29}$$

$Costs_{annual}$ is mainly associated with the operating and maintaining costs of wind and PV equipment and can be estimated according to Eq. (30).

$$Costs_{annual} = (c_{O\&M}^{wind} \times P_N^{wind}) + (c_{O\&M}^{pv} \times P_N^{pv}) \tag{30}$$

where $c_{O\&M}^{wind}$ and $c_{O\&M}^{pv}$ are the annual operating and maintaining costs per MW of rated power (US\$/MW) of the wind and the PV generation systems, respectively.

Simulation refers to analytical methods that provide solutions to several mathematical problems especially those whose modeling is complex or difficult to produce. The main characteristic of the Monte Carlo approach lays on the use of random numbers in many simulations (Flouri et al., 2015). In this paper, the cash flow and, consequently, the calculation of NPV is performed through the presented equations. MCS considers the results of Eq. (26) as an output variable and wind speed, as well as solar irradiation as input parameters. In fact, MCS utilizes random numbers to select random samples of the input data x_i associated with a given probability density function (pdf) and performs lots of simulations so that output variables y_j are generated over and over (Arnold and Yildiz, 2015). As a result, a distribution of y_j -values can be reached and transformed into probability density functions (Arnold and Yildiz, 2015). Thus, MCS can provide not only lots of random values of NPV but also the probability distribution function thereof. Through the output variables pdf, the probability of having positive NPV can be achieved, therefore, the chances of a profitable business.

According to Rout et al. (2018), 10,000 iterations are suitable for the accomplishment of stable results and the steps to carry out the Monte Carlo approach are as follows:

- (1) To calculate NPV.
- (2) To select the input variables and associate them to a pdf.
- (3) To carry out simulations with 10,000 iterations.
- (4) To obtain the pdf of the output variable: NPV.
- (5) To obtain the probability of positive NPV.

The second step is quite important. Among all variables that may influence the NPV, it is necessary being aware of those that the most affect the output. The selected ones must be associated with a probability distribution function as a rule for performing the MCS. Wais (2017) states that various studies have presented the two-parameter Weibull distribution as model to express the wind speed frequency distribution; however, the article warns that a three-parameter Weibull distribution provides better results in comparison with the two-parameter function. (Fernández Peruchena et al., 2016), in turn, suggest that annual series of solar irradiation are acceptably fitted by normal or Weibull distributions; therefore, the Weibull function is sufficient to fit wind speed datasets as well as solar irradiation data series. Eq. (31) presents the three-parameter Weibull distribution.

$$W(V_u, z, c, L) = \frac{z}{c} \left(\frac{V_u - L}{c} \right)^{z-1} e^{-\left(\frac{V_u - L}{c} \right)^z} \tag{31}$$

where V_u is the wind speed in m/s, c is the scale parameter (m/s), z is the shape parameter (a dimensionless parameter), and L is the location parameter.

Fig. 3 shows a flow chart that regards the steps performed for the achievement of the purpose of this work. The flow chart is performed for each scenario considered in this paper.

4. Energy auctions and hybrid generation systems in Brazil

The Brazilian energy market has rules that are granted and enforced by some governmental agencies, which, in turn, utilize auctions for the energy trade. Those power plant owners that offer the smallest energy tariff as means of refund for the energy provided win the auction and have the right of providing power to their clients over the period of time established in contract and by the tariff price bid for this purpose. The clients, in turn, are represented by electric power distributors, which must guarantee all the power supply requested by end-users. Since 2004, when the governmental laws altered considerably the Brazilian electric sector regulations, auctions started to be conducted to carry out power trade throughout the country and, since then, all of those wishing to sell energy in the Brazilian energy market must compete in the auctions and follow the rules of the trade. Recently, the energy market has been opened to a new model of contract, in which energy sellers may trade power to clients directly without the need to win auctions. In this form of trading, the tariff prices and the period of energy provision are agreed between the parties to the contract, that is, between the energy provider and the client. However, since the agreement is performed privately, it turns hard to obtain any information from this kind of trade and, therefore, only information from auctions are considered in this work.

The auctions are carried out publicly and all the information about the trade performed between sellers and clients are available over some communication means. Whoever accesses the governmental agencies website (ANEEL, 2019) is able to obtain some pieces of information about the lots of the Brazilian energy market auctions already run. Those pieces include: the average tariff price won in each lot of the auction, the total investment forecasted for owners to build their electric power units, the region of the country where the undertaking shall be built, the type of power generation unit, etc. Being aware of those pieces of information, as well as of some estimations made by the governmental agencies, Table 1 can be assembled, and some important variables are assumed to be worth as shown. It must be pointed out that the values of the variables presented in Table 1 are mean values of datasets obtained from several lots of wind and PV power units auctioned since 2009 and built in the region where the case study discussed in this work is sited. The total investment of each lot of electric power units auctioned in the past is divided by the total rated power of the respective undertaking so that the investment cost per each installed power is achieved.

Hybrid systems have been assembled in very recent years in Brazil and they represent a small proportion of the entire Brazilian energy generation complex. Hybrids of many different types of energy sources have been explored worldwide and lots of these systems consider PV arrangements as parts of the hybrid sets because photovoltaic systems are set up easily and do not demand large areas for installation. A few prototypes of hybrid systems started generating power around the country and have gained strength especially among hydroelectric power stations mixed with PV arrangements, as well as wind power plants and PV complexes.

In northern Brazil, specifically in Amazonas state, solar panels were placed on float boards fixed to a hydroelectric lake for extra power generation. The set of panels has 5 MW of rated power and provide

energy jointly with the hydroelectric plant. Likewise, in the north-eastern side of the country, two wind complexes in distinct areas host photovoltaic sets that produce power with wind power plants. One of these wind-PV systems has a wind power unit whose total rated power is 80 MW and whose PV set is a 11 MW-rated-power complex. The other hybrid system is used, in this work, as case study, and some information on it is discussed along the paper and utilized for the simulation of energy production from a wind-PV source.

5. Results and discussion

5.1. Case study

In order to attain the purpose of this work, a case study is presented. A hybrid wind-photovoltaic system prototype has been installed in the northeastern Brazil as a testing model for energy production. Since the region has a lack of water resources, many non-water-dependent renewables have been taken into account as a manner of generating clean and cheap energy. Caetit , a small town that hosts a hybrid complex, is one of the first places in the country to host such technological apparatus and is located at Latitude 14° 3'17" S and Longitude 42° 28'28" W. The map presented in Fig. 4 roughly shows the location of Caetit  in Brazil, as well as some pictures of the wind power plant and the PV arrangement.

Caetit  hosts a 21.6 MW-rated-power wind power plant with a 4.8 MW-rated-power PV array in a hybrid energy generation system. Although the production of energy by wind turbines is increased through PV arrays – which leads to a raise in the revenue – each type of energy source demands a initial amount of disbursement and some costs per MW of rated power. These pieces of information are important so that the technical-economic evaluation is performed comparing the viability of the complex as more or less amount of PV rated power is inserted into the hybrid system overall rated power.

The hybrid complex has eight 2.7 MW-rated-power wind turbines set in two different localities and 19,200 solar panels with 250 W of rated power each, placed in a field that is close to the site where wind power plants are located. The windmills' blades are 122 meters in diameter, while the turbines stand 89 meters tall. The PV panels are connected to four solar inverters and two transformers, which, in turn, are connected to a local substation. In addition to those inverters and transformers, the substation is also linked to the wind power plants and the overall electric energy flow provided is conducted to a larger

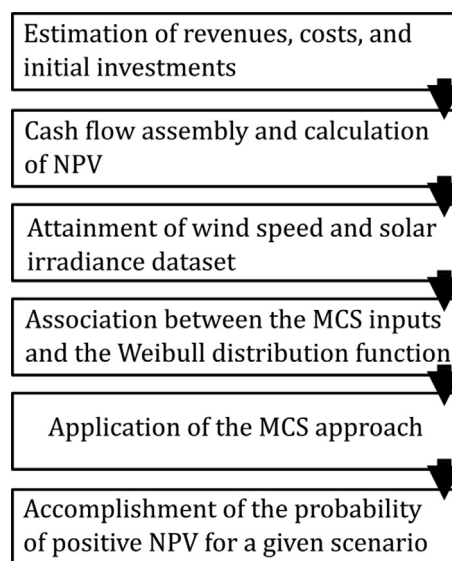


Fig. 3. Flow chart presenting the steps for accomplishment of the work analysis.

Table 1
Values of variables for the economic calculations

| Parameter | Unit of measure | Value | Source |
|-------------------|-----------------|--------------|----------------------|
| κ^{wind} | US\$/MW | 1,187,862.07 | ANEEL (2019) |
| κ^{pv} | US\$/MW | 1,656,718.51 | ANEEL (2019) |
| λ^{wind} | US\$/MWh | 45.01 | ANEEL (2019) |
| λ^{pv} | US\$/MWh | 36.43 | ANEEL (2019) |
| $c_{O\&M}^{wind}$ | US\$/MW | 26,234.57 | Energia (2016) |
| $c_{O\&M}^{pv}$ | US\$/MW | 18,981.48 | Energia (2016) |
| k | years | 20 | |
| Depreciation | years | 20 | |
| i | % | 6.99 | Aquila et al. (2016) |
| Currency | BRL/US\$ | 3.24 | |

Table 2
Caetit s’s wind speed, solar irradiance and temperature datasets obtained from MERRA and Helio-Clim 1.

| Month | Average solar irradiance, G (W/m ²) | Average insolation time, h (hours) | Average wind speed, V_u (m/s) | Average wind speed time, t_n (hours) | Average temperature, T_{amb} (  C) |
|-------|---|--------------------------------------|---------------------------------|--|--------------------------------------|
| JAN | 469.68 | 434 | 6.35 | 744 | 25.59 |
| FEV | 490.41 | 385 | 4.80 | 672 | 27.23 |
| MAR | 448.11 | 377 | 6.20 | 744 | 24.44 |
| ABR | 446.11 | 360 | 7.00 | 720 | 22.92 |
| MAI | 419.60 | 372 | 7.66 | 744 | 21.79 |
| JUN | 368.68 | 360 | 9.23 | 720 | 20.62 |
| JUL | 435.28 | 372 | 9.58 | 744 | 20.54 |
| AGO | 476.18 | 372 | 9.86 | 744 | 23.08 |
| SET | 510.82 | 379 | 10.10 | 672 | 23.06 |
| OUT | 518.46 | 403 | 9.40 | 744 | 23.76 |
| NOV | 449.78 | 390 | 6.56 | 720 | 23.24 |
| DEZ | 480.33 | 420 | 5.23 | 744 | 23.80 |

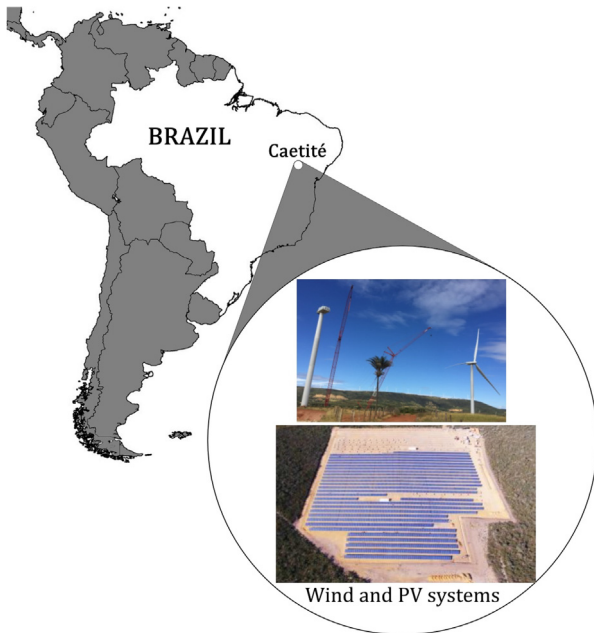


Fig. 4. Map showing Caetit s’s location and pictures of the wind and the solar complexes.

substation for power grid connection. Fig. 5 shows a sketch of the hybrid system connection.

Wind speed, solar irradiance, and temperature hourly data from the region where the hybrid system is sited are collected from January 2004 to December 2006 and a monthly average is reached. Further, the monthly average time in which solar irradiation is locally provided is also attained so that the energy generated by PV panels can be calculated. Table 2 presents those pieces of information. Wind blows 24 h a day so the monthly time considered in this work for the wind energy production corresponds to the number of days of a certain month multiplied by 24 h. From the data collection, parameters of the Weibull function may be obtained. For each month of the year, different parameters’ values are considered since the datasets are distinct each month. Table 3 brings the Weibull distribution parameters’ values attained monthly for wind speed and solar irradiation datasets.

Several types of power sources form an integrated system that have been connected to each other differently and have been generically denominated as hybrid systems. Despite this technology is very recent in Brazil, governmental bodies and agencies have already classified the types of integrated systems according to the sort of connection they have and the level of contract. Among some terms used by such governmental bodies, *associated* and *hybrid* are designed to classify power

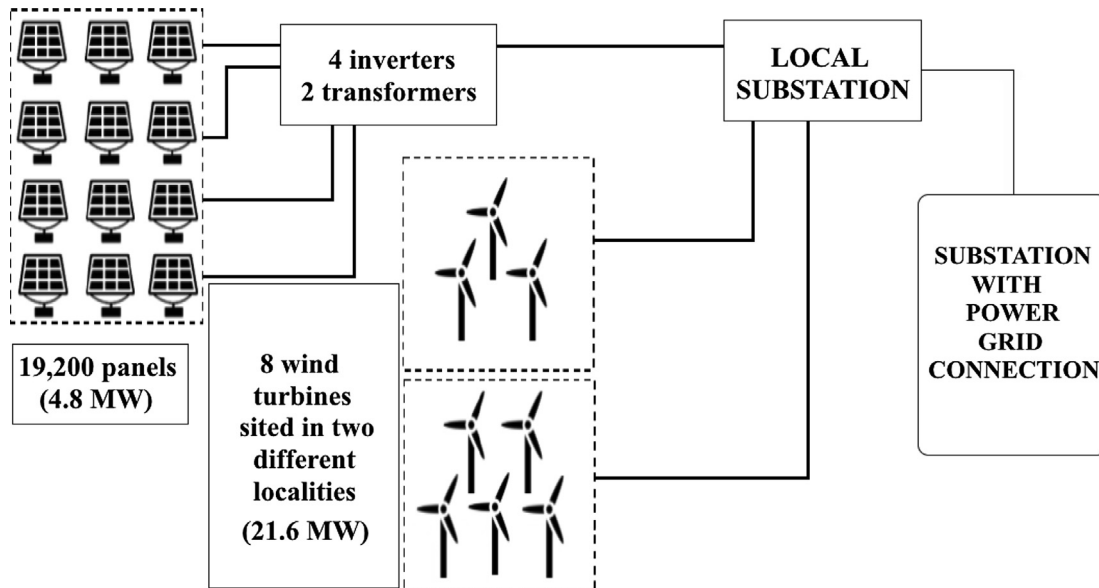


Fig. 5. Sketch of the hybrid energy system.

Table 3
Parameters of the Weibull distribution for the wind speed and the solar irradiation datasets

| Month | Function | Wind Speed c;z:L | Solar irradiation c;z:L |
|-------|----------|-----------------------|----------------------------|
| JAN | Weibull | 8.23;3.20;-1.02 | 3671.08;50.15;-3160.58 |
| FEB | Weibull | 10.07;4.18;-4.35 | 1998.79;28.10;-1486.09 |
| MAR | Weibull | 6.13;3.48;0.68 | 478.81;4.02;13.22 |
| APR | Weibull | 7.95;4.292;-0.24 | 463.13;6.46;14.04 |
| MAY | Weibull | 7.72;3.52;0.71 | 429.29;5.06;0.3 |
| JUN | Weibull | 57.37;41.06;-47.36 | 427.18;6.70;-30 |
| JUL | Weibull | 7.10;4.58;3.09 | 671.47;11.77;-233.51 |
| AUG | Weibull | 181.39;107.72;-170.57 | 40,989.95;999;-40,490.12 |
| SEP | Weibull | 14.64;7.03;-3.53 | 2893.13;46.20;-2.368.91 |
| OCT | Weibull | 14.88;6.90;-4.51 | 577.03;4.35;-44.18 |
| NOV | Weibull | 12.09;3.75;-4.36 | 398.55;2.38;87.74 |
| DEC | Weibull | 10.57;5.42;-4.51 | 860.97;8.49;-332.78 |

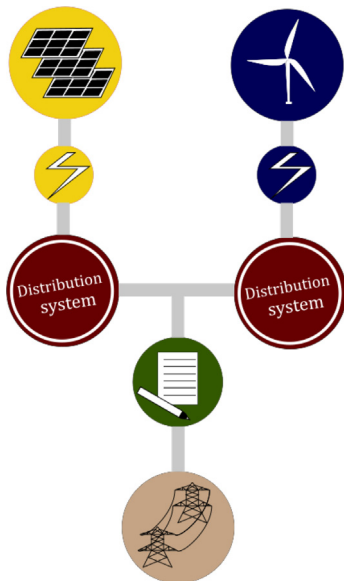


Fig. 6. Sketch of the system connection.

Table 4
Scenarios table.

| | Wind rated power (MW) | PV rated power (MW) | Proportion of wind rated power to the overall system | Proportion of PV rated power to the overall system |
|-------------|-----------------------|---------------------|--|--|
| Scenario 1 | 26.40 | 0.00 | 100.0% | 0.0% |
| Scenario 2 | 23.76 | 2.64 | 90.0% | 10.0% |
| Scenario 3 | 22.44 | 3.96 | 85.0% | 15.0% |
| Scenario 4* | 21.60 | 4.80 | 81.8% | 18.2% |
| Scenario 5 | 19.80 | 6.60 | 75.0% | 25.0% |
| Scenario 6 | 18.48 | 7.92 | 70.0% | 30.0% |
| Scenario 7 | 17.16 | 9.24 | 65.0% | 35.0% |
| Scenario 8 | 15.84 | 10.56 | 60.0% | 40.0% |
| Scenario 9 | 14.52 | 11.88 | 55.0% | 45.0% |
| Scenario 10 | 13.20 | 13.20 | 50.0% | 50.0% |
| Scenario 11 | 11.88 | 14.52 | 45.0% | 55.0% |
| Scenario 12 | 10.56 | 15.84 | 40.0% | 60.0% |

* Case study scenario.

systems of integrated generation.

Associated systems comprise those that share the same area, connections infrastructure, and power grid access; however, in this configuration, each type of source generates its power independently. Hybrid systems, in turn, are those whose combination still occurs in the energy production process, and, specifically for wind-and-PV-hybrid-

complexes, both of the types of sources utilize the same conversion system (Ponte, 2019). Although this terminology is defined for the context of the Brazilian energy market, this work employs the term *hybrid* as generic terminology for power systems of integrated generation. Fig. 6 shows a sketch of the connection of the case study system. Because the converter is not the same for both of the types of power sources, the system configuration is set as the associated system defined by governmental bodies. In other words, in the configuration of the case study system, it is found that each power source generates electric power separately from one another, but they share the distribution system contractually.

5.2. Scenarios and results

Some hypothetical scenarios are introduced in this work so that the financial feasibility of the insertion of PV arrays into wind power plants may be verified. Each scenario sets different wind-and-PV-rated-power values, which allows an evaluation of how the power generation from solar arrays affects the wind energy production economically. The scenarios are taken by considering the overall amount of rated power in the real hybrid system, that is, the proportion taken in each scenario is based on the total of 26.4 MW, which is the sum of the wind complex rated power – 21.6 MW – and the PV array rated power – 4.8 MW – found in the hybrid system of the case study. It is chosen twelve scenarios randomly in such a way that the first one comprises a 100%-wind-power-plant with no PV power installed. The others have the wind power percentage decreased proportionally to the increase of PV power as the scenarios are presented. Twelve scenarios are adequate for this study since the probability of positive NPV is equal to zero for scenarios beyond the twelfth. Table 4 shows the configuration of each scenario. Scenario 4 brings the characteristics of the case study analyzed in this work. Fig. 7, in turn, shows the probability of positive NPV for each scenario regarded, with the x-axis representing the scenarios and the y-axis showing the likelihood of positive NPV occurrence.

A positive NPV implies a profitable business. The graph shows, therefore, the probability of a feasible undertaking as more or less PV array system is inserted into the hybrid complex. A pure wind energy system is the ideal hybrid set with 98% probability that a positive NPV occurs. As PV arrays are inserted into the complex, the chances of a successful business decreases, although it does not become unfeasible if low quantity of PV rated power is utilized. In the case study, whose proportion of PV rated power to the overall rated power is 18.2%, the probability of positive NPV remains quite high reaching 89%. However, the more PV arrays are added in the generation system, the more unprofitable becomes the energy generation undertaking. Further, from a 65%-35% configuration to a continuous increase of PV power insertion, it is notable a riskier undertaking in which the owner may not have economic returns. Once the hybrid system is comprised of 60% of PV power, there are no chances to obtain a lucrative business.

In order to assess the power generation by each energy source, the capacity factors of the wind power plant and the PV arrangement of the case study are calculated through Eq. (15) and (25), as well as by using the information presented in the case study and in Table 2. As a result, cf_{annual}^{wind} is found to be equal to 50.9%, which is approximately in accordance with MME (2017) that shows a wind capacity factor of 42% for the whole country in 2016. On the other hand, cf_{annual}^{pv} is calculated and equal to 20.1%. Proportionally, the wind power plants are broadly more efficient than the PV system as is evidenced by the *cf* found for each type of source.

6. Conclusion

A technical-economic risk study is carried out in this work to assess the financial impact of the PV power insertion into a wind energy system. The analysis is performed considering a wind-PV hybrid system, and the methodology utilized for the economic evaluation comprises

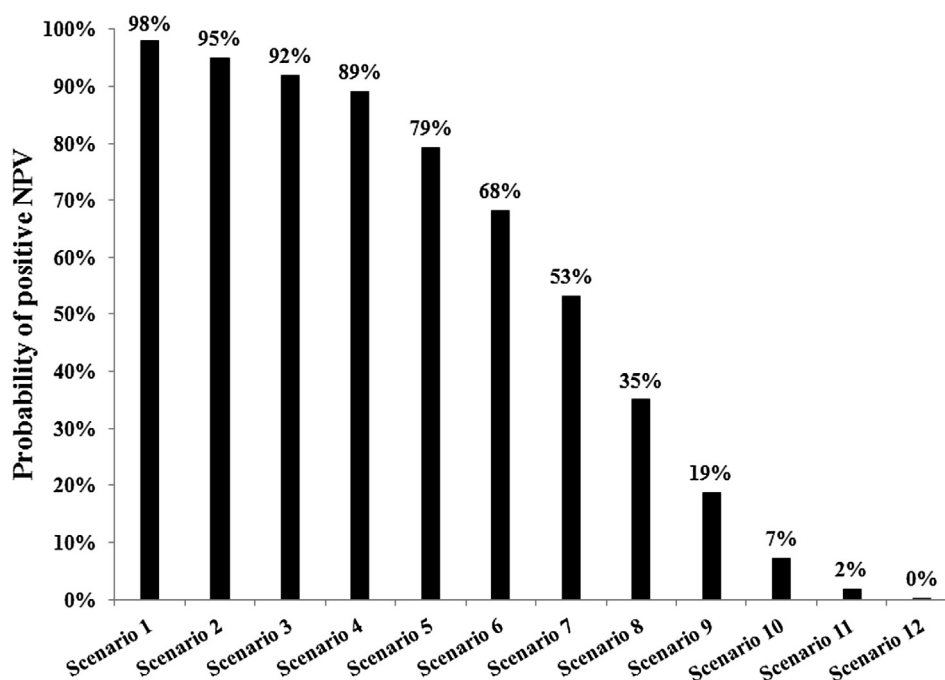


Fig. 7. The probability of the positive NPV occurrence.

the NPV as a financial analysis tool, as well as the MCS as a stochastic approach due to the probabilistic nature of the variables considered.

The results show that the ideal economic scenario comprises a pure wind power plant, and a constant increase of PV power into wind power plants causes a decrease in the probability of positive NPV. In other words, as the hybrid energy system presents increasingly photovoltaic resources, less economically attractive becomes the energy generation business. It occurs mainly because PV power devices are still rather expensive compared to wind source equipment and, therefore, high initial investment costs are required in order to acquire PV arrays, whereas a lower capital is needed to purchase equivalent rated power of wind sources. In addition, the capacity factors calculated for each type of source showed that the PV system provides fairly low energy proportionally to what it could provide running at maximum power, while the wind power plants present a greater capacity factor compared to the solar power unit. Thus, we may notice that photovoltaic farms cause low financial returns to owners since large scale solar systems are still expensive in Brazil and, despite the abundance of solar resources, the production of power by PV systems is proportionally rather low in comparison to wind power generation units.

Nevertheless, the undertaking considered still maintains a high probability of being successful for certain amount of PV-rated-power placed in the complex. In the case study, for example, in which the hybrid system consists of 81.8% of wind-rated-power and 18.2% of PV-rated-power, the probability of a profitable business reaches 89% roughly, which demonstrates that the undertaking maintains a high probability of being successful with some PV power installed. With respect to the applied methodology, NPV and MCS demonstrated that they are powerful tools in economic analysis of renewable energy systems contributing toward the attainment of the purpose of this work.

Declaration of Competing Interest

The authors declare that there is no conflict of interests regarding the publication of this paper.

Acknowledgment

The authors would like to acknowledge CAPES for the financial

support for this research.

References

- Aguilar-jiménez, J.A., Velázquez, N., Acuña, A., Cota, R., González, E., González, L., 2018. Techno-economic analysis of a hybrid PV-CSP system with thermal energy storage applied to isolated microgrids. *Sol. Energy* 174 (May), 55–65. <https://doi.org/10.1016/j.solener.2018.08.078>.
- Al-ghussain, L., Ahmed, H., Haneef, F., 2017. Optimization of hybrid PV-wind system: case study Al-Tafilah cement factory. *Jordan* 2018 (30), 24–36. <https://doi.org/10.1016/j.seta.2018.08.008>.
- Almeida, M.P., Muñoz, M., de la Parra, I., Perpiñán, O., 2017. Comparative study of PV power forecast using parametric and nonparametric PV models. *Sol. Energy* 155, 854–866. <https://doi.org/10.1016/j.solener.2017.07.032>.
- Alramlawi, M., Gabash, A., Mohagheghi, E., Li, P., 2017. Optimal operation of hybrid PV-battery system considering grid scheduled blackouts and battery lifetime. *Sol. Energy* 2018 (161), 125–137. <https://doi.org/10.1016/j.solener.2017.12.022>.
- Andini, C., Cabral, R., Santos, J.E., 2019. The macroeconomic impact of renewable electricity power generation projects Eus e. *Renew. Energy* 131, 13. <https://doi.org/10.1016/j.renene.2018.07.097>.
- ANEEL, 2019. LEILÕES. 2019. <http://www.aneel.gov.br/resultados-de-leiloes>.
- Aquila, G., Rocha, L.C.S., Rotela Junior, P., Pamplona, E.d.O., de Queiroz, A.R., de Paiva, A.P., 2016. Wind power generation: an impact analysis of incentive strategies for cleaner energy provision in Brazil. *J. Cleaner Prod.* 137, 1100–1108. <https://doi.org/10.1016/j.jclepro.2016.07.207>.
- Aquila, G., Rotela Junior, P., de Oliveira Pamplona, E., de Queiroz, A.R., 2017. Wind power feasibility analysis under uncertainty in the Brazilian electricity market. *Energy Econ.* 65, 127–136. <https://doi.org/10.1016/j.eneco.2017.04.027>.
- Arnold, U., Yildiz, O., 2015. Economic risk analysis of decentralized renewable energy infrastructures e A Monte Carlo Simulation approach. *Renew. Energy* 77, 227–239. <https://doi.org/10.1016/j.renene.2014.11.059>.
- Barbieri, F., Rajakaruna, S., Ghosh, A., 2016. Very short-term photovoltaic power forecasting with cloud modeling: a review. *Renew. Sustain. Energy Rev.* 2017 (75), 242–263. <https://doi.org/10.1016/j.rser.2016.10.068>.
- Blanco, S., Caliot, C., Cornet, J.F., Coustet, C., Meilhac, N., Pajot, A., Paulin, M., Perez, P., Piaud, B., Roger, M., Rolland, J., 2014. Monte Carlo advances and concentrated solar applications 103, 653–681. <https://doi.org/10.1016/j.solener.2013.02.035>.
- Boccard, N., 2009. Capacity factor of wind power realized values vs. estimates. *Energy Policy* 37, 2679–2688. <https://doi.org/10.1016/j.enpol.2009.02.046>.
- Boilley, A., Wald, L., 2015. Comparison between meteorological re-analyses from ERA-Interim and MERRA and measurements of daily solar irradiation at surface. *Renew. Energy* 75, 135–143. <https://doi.org/10.1016/j.renene.2014.09.042>.
- Daigavane, M.B., Fulzele, J.B., 2018. Design and optimization of hybrid PV-wind renewable energy. *Mater. Today: Proc.* 5, 9. <https://doi.org/10.1016/j.matpr.2017.11.151>.
- Ding, Z., Hou, H., Yu, G., Hu, E., Duan, L., Zhao, J., 2019. Performance analysis of a wind-solar hybrid power generation system. *Energy Convers. Manage.* 181, 1–12. <https://doi.org/10.1016/j.enconman.2018.11.080>.
- Elibol, E., Ozmen, T.O., Tutkun, N., Koysal, O., 2016. Outdoor performance analysis of

- different PV panel types. *Renew. Sustain. Energy Rev.* 651–661, URL.
- Energia, E.P.E., 2016. Renovável: hidráulica, biomassa, eólica, solar, oceânica. EPE, Rio de Janeiro.
- Feretic, D., Tomsic, Z., 2005. Probabilistic analysis of electrical energy costs comparing: production costs for gas, coal and nuclear power plants. *Energy Policy* 33 (1), 5–13. [https://doi.org/10.1016/S0301-4215\(03\)00184-8](https://doi.org/10.1016/S0301-4215(03)00184-8).
- Fernández, E.F., Almonacid, F., Rodrigo, P., Pérez-Higueras, P., 2013. Model for the prediction of the maximum power of a high concentrator photovoltaic module. *Sol. Energy* 97, 12–18. <https://doi.org/10.1016/j.solener.2013.07.034>.
- Fernández Peruchena, C.M., Ramírez, L., Silva-Pérez, M.A., Lara, V., Bermejo, D., Gastón, M., Moreno-Tejera, S., Pulgar, J., Liria, J., Macías, S., Gonzalez, R., Bernardos, A., Castillo, N., Bolinaga, B., Valenzuela, R.X., Zorzalejo, L.F.A., 2016. statistical characterization of the long-term solar resource: towards risk assessment for solar power projects. *Sol. Energy* 123, 29–39. <https://doi.org/10.1016/j.solener.2015.10.051>.
- Flouri, M., Karakosta, C., Kladouchou, C., Psarras, J., 2015. How does a natural gas supply interruption affect the EU gas security? A Monte Carlo simulation. *Renew. Sustain. Energy Rev.* 44, 785–796. <https://doi.org/10.1016/j.rser.2014.12.029>.
- Fuentes, M., Nofuentes, G., Aguilera, J., Talavera, D.L., Castro, M., 2007. Application and validation of algebraic methods to predict the behaviour of crystalline silicon PV modules in Mediterranean climates. *Sol. Energy* 81 (11), 1396–1408. <https://doi.org/10.1016/j.solener.2006.12.008>.
- Gu, Y., Zhang, X., Are, J., Han, M., Chen, X., Yuan, Y., 2018. Techno-economic analysis of a solar photovoltaic/thermal (PV/T) concentrator for building application in Sweden using Monte Carlo method. *Energy Convers. Manage.* 165 (January), 8–24. <https://doi.org/10.1016/j.enconman.2018.03.043>.
- Heck, N., Smith, C., Hittinger, E., 2016. A Monte Carlo approach to integrating uncertainty into the levelized cost of electricity. *Electr. J.* 29 (3), 21–30. <https://doi.org/10.1016/j.tej.2016.04.001>.
- Huang, Q., Shi, Y., Wang, Y., Lu, L., Cui, Y., 2015. Multi-turbine wind-solar hybrid system. *Renew. Energy* 76, 401–407. <https://doi.org/10.1016/j.renene.2014.11.060>.
- Ishaq, H., Dincer, I., Naterer, G.F., 2018. Development and assessment of a solar, wind and hydrogen hybrid trigeneration system. *Int. J. Hydrogen Energy* 43, 1–13. <https://doi.org/10.1016/j.ijhydene.2018.10.172>.
- Kim, C.K., Kim, H.G., Kang, Y.H., Yun, C.Y., Kim, S.Y., 2019. Probabilistic prediction of direct normal irradiance derived from global horizontal irradiance over the Korean Peninsula by using Monte-Carlo simulation. *Sol. Energy* 180 (January), 63–74. <https://doi.org/10.1016/j.solener.2019.01.030>.
- Krozer, Y., 2013. Cost and bene fit of renewable energy in the European Union. *Renew. Energy* 50, 68–7. <https://doi.org/10.1016/j.renene.2012.06.014>.
- Kulunk, E., 2011. Aerodynamics of wind turbines. In: *Fundamental and Advanced Topics in Wind Power*. IntechOpen, USA. <https://www.intechopen.com/books/fundamental-and-advanced-topics-in-wind-power>. doi:10.5772/731.
- Lamas, W.d.Q., 2017. Exergo-economic analysis of a typical wind power system. *Energy* 140, 1173–1181. <https://doi.org/10.1016/j.energy.2017.09.020>.
- Lee, J., Chang, B., Aktas, C., Gorthala, R., 2016. Economic feasibility of campus-wide photovoltaic systems in New England. *Renew. Energy* 99, 452–464. <https://doi.org/10.1016/j.renene.2016.07.009>.
- Lefèvre, M., Blanc, P., Espinar, B., Gschwind, B., Ménard, L., Ranchin, T., Member, S., Wald, L., Saboret, L., Thomas, C., 2014. The HelioClim-1 database of daily solar radiation at earth surface: an example of the benefits of GEOS data-CORE. *IEEE J. Sel. Top. Appl. Earth Observ. Remote Sens.* 7 (5), 1745–1753. <https://doi.org/10.1109/JSTARS.2013.2283791>.
- Lorenzo, E., 1994. *Solar Electricity – Engineering of Photovoltaic Systems*. PROGENSA, Sevilla.
- Marion, B., 2002. A method for modeling the current-voltage curve of a PV module for outdoor conditions. *Prog. Photovoltaics Res. Appl.* 10 (3), 205–214. <https://doi.org/10.1002/ppp.403>.
- Martins, F.R., Pereira, E.B., Abreu, S.L., 2007. Satellite-derived solar resource maps for Brazil under SWERA project. *Sol. Energy* 81, 517–528. <https://doi.org/10.1016/j.solener.2006.07.009>.
- Middleton, P., 2018. Sustainable living education: techniques to help advance the renewable energy transformation. *Sol. Energy* 174 (October), 1016–1018. <https://doi.org/10.1016/j.solener.2018.08.009>.
- MME M.d.M.e.E. Energia eólica no Brasil e no mundo. 2017. URL <http://www.mme.gov.br/documents/10584/3580498/15+-+Energia+Eólica+-+Brasil+e+Mundo+-+ano+ref.+2016+%28PDF%29+-+NOVO/f63a15ea-9d2c-4d27-9400-5d7c3fd97b22?version=1.4>.
- Olauson, J., Bergkvist, M., 2015. Modelling the Swedish wind power production using MERRA reanalysis data. *Renew. Energy* 76, 717–725. <https://doi.org/10.1016/j.renene.2014.11.085>.
- Osterwald, C.R., 1986. Translation of device performance measurements to reference conditions*. *Sol. Cells* 18, 269–279.
- Pillot, B., de Siqueira, S., Dias, J.B., 2018. Grid parity analysis of distributed PV generation using Monte Carlo approach: the Brazilian case. *Renew. Energy* 127, 974–988. <https://doi.org/10.1016/j.renene.2018.05.032>.
- Ponte, G., 2019. Usinas híbridas no Sistema Interligado Nacional. 2019. URL http://epe.gov.br/sites-pt/sala-de-imprensa/noticias/Documents/apresentacao_EPE.pdf.
- Rocha, L.C.S., Aquila, G., Pamplona, E.d.O., de Paiva, A.P., Chieregatti, B.G., Lima, J.d.S.B., 2017. Photovoltaic electricity production in Brazil: a stochastic economic viability analysis for small systems in the face of net metering and tax incentives. *J. Cleaner Prod.* 168, 1448–1462. <https://doi.org/10.1016/j.jclepro.2017.09.018>.
- Ross, R., Smokler, M., 1986. Flat-Plate Solar Array Project. *Eng. Sci. Reliab.* 6.
- Rout, A., Sahoo, S., Thomas, S., 2018. Risk modeling of domestic solar water heater using Monte Carlo simulation for east-coastal region of India. *Energy* 145, 548–556. <https://doi.org/10.1016/j.energy.2018.01.018>.
- Shadmehri, M., Narei, H., Ghasempour, R., Behshad, M., 2018. Numerical simulation of a concentrating photovoltaic-thermal solar system combined with thermoelectric modules by coupling Finite Volume and Monte Carlo Ray-Tracing methods 172 (July), 343–356. <https://doi.org/10.1016/j.enconman.2018.07.034>.
- Spiru, P., Lizica-simona, P., 2018. Technical and economical analysis of a PV/wind/diesel hybrid power system for a remote area. *Energy Procedia* 147, 343–350. <https://doi.org/10.1016/j.egypro.2018.07.102>.
- Syed, I.M., 2017. Near-optimal standalone hybrid PV/ WE system sizing method. *Sol. Energy* 157 (July), 727–734. <https://doi.org/10.1016/j.solener.2017.08.085>.
- Villalva, M.G., Gazoli, J.R., Filho, E.R., 2009. *Comprehensive Approach to Modeling and Simulation of Photovoltaic Arrays* 24 (5), 1198–1208.
- Wais, P., 2017. Two and three-parameter Weibull distribution in available wind power analysis. *Renew. Energy* 103, 15–29. <https://doi.org/10.1016/j.renene.2016.10.041>.
- Xi, X., Ignatov, A., Zhou, X., 2019. Remote sensing of environment exploring MERRA-2 global meteorological and aerosol reanalyses for improved SST retrieval. *Remote Sens. Environ.* 223 (January), 1–7. <https://doi.org/10.1016/j.rse.2019.01.011>.
- Yan, J., Ouyang, T., 2018. Advanced wind power prediction based on data-driven error correction. *Energy Convers. Manage.* 2019 (180), 302–311. <https://doi.org/10.1016/j.enconman.2018.10.108>.